Lecture 10: Time/Space noise and « thermal » processing of temperature signal

JC Batsale, C Pradere

TREFLE-I2M, Esplanade des Arts et Métiers, 33405 Talence, France
E-mail: Jean-Christophe.batsale@ensam.eu

Abstract. This text proposes simple methods for the processing of time and space temperature fields such as the fields provided by infrared thermography devices, for the non-destructive evaluation of heterogeneous samples. A first part is devoted to noise considerations and the possible errors coming from the instrument and the experimental situation. The second part is concerning the estimation of fields of thermophysical properties from space-time fields of temperatures. As illustration examples, the space derivative of the signal and the local estimation of thermal diffusivity fields are analyzed in the case of 1D transverse or in-plane diffusion. The main strategies consist in projecting the space-time signal in a suitable basis of functions, nevertheless other strategies such as considering the correlation between space laplacian and time derivative of the observable field, can be useful even if the signal is very noisy.

0.Introduction

The processing of space and time temperature fields is more and more necessary because devices are now currently available in order to quickly measure, store and process thermal information. Infrared thermography devices are the most usual. But a lot of other possibilities with contact or non-contact sensors (with optical or mechanical scans) will appear in the future and a lot of questions about “how to process” and “how to estimate” thermophysical properties from such fields are now posed.

It is here proposed to review some of the difficulties occurring with such instruments and how to overcome them.

The first part will be devoted to the analysis of the noise and signal perturbation from such kind of “space-time” sensors.

A 2D temperature field can be the signature of a lot of heat transfer phenomena at the surface of a solid or a liquid (heat conduction or diffusion through homogeneous or heterogeneous media, convective transport in complex systems,…). One of the main intuitive way to process the signal is to study the time or space derivatives of such fields, in order to link the temperature observation to a heat transfer model. The second part of this text will illustrate on simple examples, some ways and difficulties related to the derivations of the signals and the estimation of thermophysical properties with regards to the general heat transfer equation.

1. Noise and signal perturbation from temperature sensors

1.1 Characterization of time/space noise, depending on the measurement device:
1-1-1 Monosensor

In the past (only 30 years ago!), only one measurement generally at steady state was related to a very expensive and technological experiment. The guarded hot plate was the emblematic example of such devices, in order to estimate the thermal conductivity of a homogeneous sample. In such devices, only one or two temperature measurements were implemented and “hand-controlled” for maintaining the steady-state regime.

Now, millions of thermal data related to simple experiments are available from infrared cameras or optical and mechanical devices. It is necessary to examine the characteristics of such devices and to analyze the validity of the signals, but first keep in mind that the enormous amount of data is advantageous since the computational effort related to such data is reduced.

Generally a monosensor (thermocouple/ electrical resistance, quantum detector, photomultiplier…) is giving a regularly time-spaced information coming from a complex unknown electronic chain (amplifier, analogical/numerical converter, filters, ….). It is instructive to observe (as far as possible) a stationary signal (trying to avoid any perturbation) coming from a measurement chain, in order to intuitively set out some characteristics. The figure 1 is illustrating several situations often encountered (gaussian noise, periodic parasite, correlated signal, digitization noise…). Such noise, in the different situations of figure 1, has a zero mean and a quite uniform standard deviation, even if the fundamental nature of the noise is not the same.

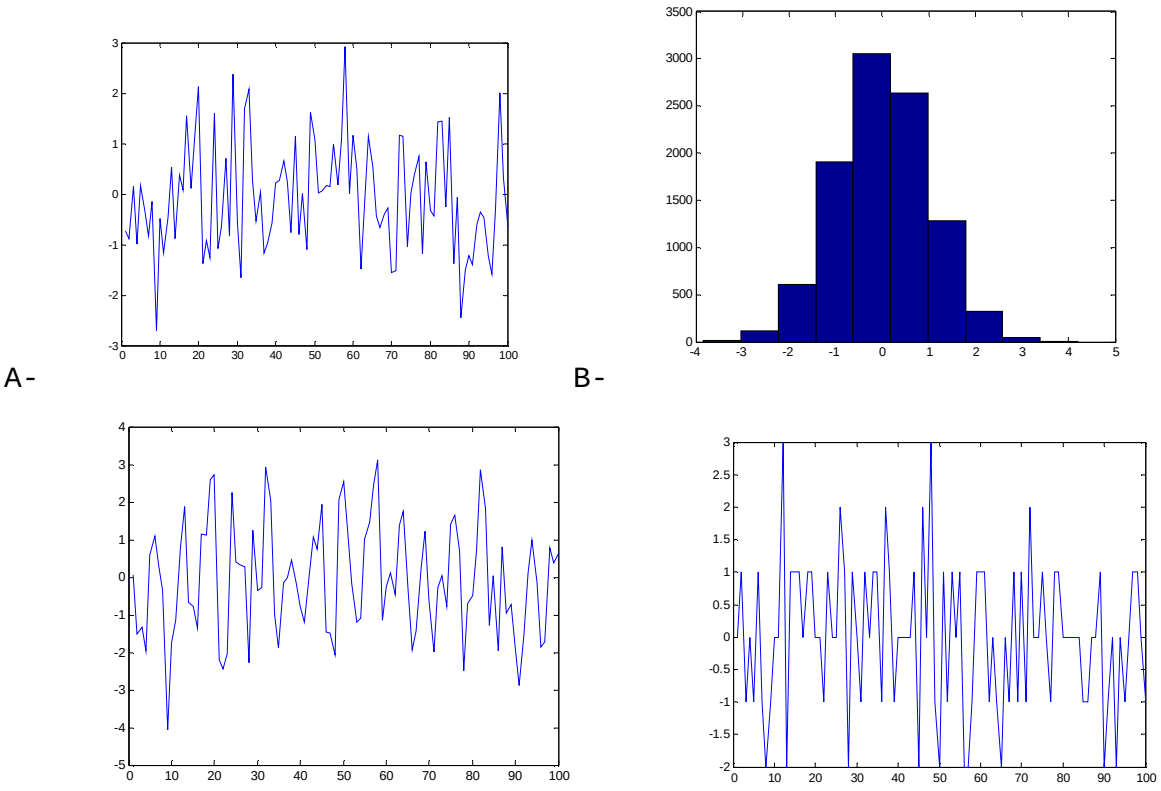

A- B-

C- D-

Figure 1: several noise illustrations from a monosensor (A-random signal, B-histogram of A- with 10000time steps (instead of 100 in fig A-), C- parasitic periodic noise superposed to the signal, D-Digitization noise from A)

For practical reasons, the noise associated to the real signal vector $\hat{\mathbf{Y}}$ of a monosensor will be considered as an undesired random fluctuation (random variable: $\mathbf{e}_Y$) which is added

to a signal $\mathbf{Y}$ (even distorted and biased) coming the physical phenomenon of interest, such as:

$$\hat{\mathbf{Y}} = \mathbf{Y} + \mathbf{e}_Y$$

The main characteristics of a monosensor is generally the noise amplitude (or the standard deviation of $\mathbf{e}_Y$) and the mean value which is assumed to be zero ($E(\hat{\mathbf{Y}}) = E(\mathbf{Y})$---> $E(\mathbf{e}_Y) = 0$).(with $E(\,)$: expected value operator). The signal to noise ratio is generally the ratio between the standard deviation and the mean value.
Generally, it is assumed that the error on $\mathbf{Y}$ has a constant standard deviation σ □□such as :

$$\text{cov}\,(\mathbf{e}_Y) = \sigma^2 \mathbf{I}$$

1.1.2 Sensor array
Since the years 2000, the infrared cameras are offering signals form a focal plane array of detectors which gives at the same time not only one signal but a matrix of signals coming from all the detectors with different characteristics. The consideration of the whole matrix of detectors as uniform is a dangerous assumption and instead of one mean value and one standard deviation, it is suitable to consider the covariance matrix of the array (very often and because it is simpler, the covariance of the array will be considered as uniform as the covariance of a monosensor, such as: cov $(\mathbf{e}_Y) = \sigma^2 \mathbf{I}$).

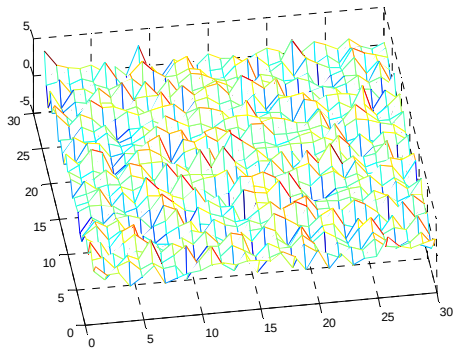

A-

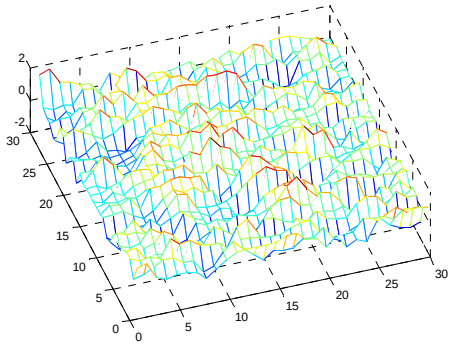

B-

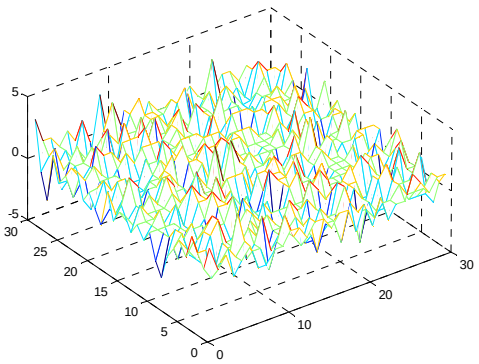

C-

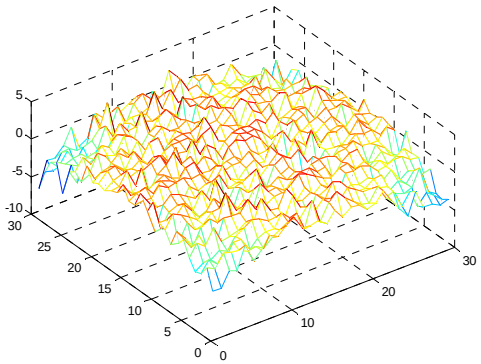

D-

Figure 2; Examples of noise occurring with a 2D array of sensors, A- random Gaussian, B- non-isotropic spatial correlation, C- Digitized noise D-Non-uniformity distortion

1.2 Examples of systematic errors with thermocouples and IR cameras
1.2.1 Inertia and position errors with contact monosensors

Even if the previous random noise is undesired, the properties of the mean value and the knowledge of the variance, standard deviation or covariance matrix allow to process the signal. Unfortunately, systematic errors can also occur and introduce a non-detectable error.
A thermocouple is a solid sensor which is perturbating the temperature field especially when high temperature gradients are implemented. Even if several precautions are taken such as putting the sensor and the connection wire along the assumed isotherm curve or plane, the inertia in the case of transient experiment cannot be avoided (see [1]). Generally the output signal of the sensor is considered as a convolution product which take into account the thermal contact resistance or an exchange coefficient h and an apparent heat capacity ρcL for the system such as:

$$Y(t) = \frac{K}{\rho cL}\int_0^t \exp\left(-\frac{h}{\rho cL}\tau\right)U(t-\tau)d\tau = \int_0^t H(\tau)U(t-\tau)d\tau = \int_0^t H(t-\tau)U(\tau)d\tau$$

K is an arbitrary multiplicative constant and $U(t)$ is the idealized signal without inertia and the inertial and resistance effects can be represented under an impulsional response: $H(t)$.
The implementation of the previous expression needs often a discretization and can be presented as:

$$Y_i = \sum_{j=1}^{i} H_{i-j}U_j\Delta t \qquad \text{or} \qquad \begin{bmatrix} Y_1 \\ Y_2 \\ . \\ . \\ Y_m \end{bmatrix} = \Delta t \begin{bmatrix} H_1 & 0 & & & 0 \\ H_2 & H_1 & 0 & & \\ H_3 & H_2 & H_1 & & \\ . & . & & . & 0 \\ H_m & H_{m-1} & & H_2 & H_1 \end{bmatrix} \begin{bmatrix} U_1 \\ U_2 \\ . \\ . \\ U_m \end{bmatrix}$$

One way to avoid such difficulties is to estimate the transfer function between the measured temperature response and a surface heat flux which causes the transient gradient. A prerequisite condition is to be able to excite the system with a calibrated heat flux and to estimate from a model the impulse response or the transfer function (see [2]).

1.2.2 Some examples of systematic errors with sensor-arrays,(Calibration, non uniformity of a detectors array, bad pixels, dead time...)

-Calibration, emission and reflexion
In the case of infrared cameras, the systematic errors are not coming from the inertia or the thermal resistances (only with contact solid sensors) but from the calibration of the great amount of radiative sensors and the estimation of the radiative balance between the sensor (proper emission, reflexion and influence of the environment) (see [3], [4]). The Luminance coming from the observed surface is a function of the temperature of the object (Planck's law) and must be calibrated previously with a black body source. Such calibration is a source of systematic error (non linearities, emissivity,..) which will be here assumed to be overcome.
If the influence of the atmosphere between the camera and the measured surface is considered as perfectly transparent, the measured luminance is then considered as only depending on the proper emission of the surface and the reflection of the environment.
In order to avoid the parasitic effects of the reflexion, it is convenient to study the transient temperature response of the surface of a system to a calibrated even localised heating (see [5]).

-Non-Uniformity Correction

The infrared cameras are generally sold with a pre-calibration system of the pixels, A distribution of gain and offset for each pixel must be regularly re-estimated (Non Uniformity Correction). The estimation is generally obtained from the measurement of the emission of an isothermal surface at two different temperatures (generally with an extended blackbody). Sometimes, these distributions are corrected by the internal temperature of the camera in order to take into account the time derive of the environment or the electronic system.
Then the relationship between the measured heat flux (measured luminance) is related to the temperature of the observed surface by a global calibration (estimation of Planck law parameters or of polynomial parameters fitting the Planck Law).

-Bad or dead Pixels

Out of the non-uniformity correction, the detector array can present defects such as bad or dead pixels (less than 0.5%). Generally, these pixels are recognized initially by the device provider and corrected by a signal averaged from the neighbouring pixels (Bad Pixel Replacement).

-Time recording, dead time step

One other important defect related to the infrared cameras consists in the *dead time* detections. Even if the recording of frames is assumed to be at regularly spaced time steps it is necessary to examine the real time recording steps provided by the last generation of thermographic devices (see [5]). In fact, a lot of delays have to be considered in a thermographic device.
The *integration time* is the delay for the recording of the radiation emitted by the considered surface, by the detector. The detectors of the array are recording simultaneously the thermal scene (*snapshot mode*) and therefore the integration time is the time resolution limit of the device. The electronic transfer of the informations from the detectors to the storage memory is then insured with a delay (*electronic transfer delay*) generally much longer than the integration time (several ms instead of several µs). This characteristic is important because for fast phenomena observation (or fast apparent scanning) the electronic transfer can fail and give irregular recording time steps. It is then more advantageous to implement a high frequency periodic phenomenon and to record the images with a trigger controled at stroboscopic frequencies (see [6]). In all cases, if the recording time is not perfectly controlled, the errors induced, for instance, with a time derivation of the signal will be strongly different from the classical random noise assumption since the time is considered as an explicative variable (known without errors…). Generally this phenomenon is not affecting the visualization of the thermal phenomenon, but the processing (see [7]).

-Thermal stability of the instrument
The stability of the signal delivered by the infrared camera is often related to the internal temperature of the detector array which is about 80°K. Unfortunately the freezing of the detector array and the thermal regulation is not always stable (1 to 5 mK). This instability is influencing the nominal properties of the detector array and consequently the Non Uniformity Correction.
By the same way, the detector array is an energetic system influenced by the internal heat pump and also by the external ambient temperature conditions.

-Space resolution
The apparent number of pixels of an image is not a sure indication about the space resolution. With the ancient thermographic devices, the image was built with an optical

scanning and a single detector. Very often the scanning was inducing an “overlapping” of the pixels and a strong spatial correlation acting as a space convolution effect (or blurring effect) of the image dramatically damaged by the absence of possibility of snapshot mode (time lag for each pixel).
The effects of such “pixel correlation” are attenuated with a focal plane array of detectors and then improving the image resolution (or the apparent image quality). Nevertheless, the examination of the correlation of the pixels with the neighbors remains necessary. A classical test is the slit response function measurement.

A cool slit (at *Tslit*) with a variable width x is placed in front of a hot plate at *Tplate*. The width of the slit is varied in order to obtain the Slit Response Function (*SRF(x)*) such as :

$$SRF(x) = \frac{T(x) - Tslit}{Tplate - Tslit},$$

Such a function is corresponding with symmetry considerations to a step response see figure 3.
It means that the image signal is convoluted with the derivative of the SRF. (see figure 3). Generally the characteristic width of the is about 2 or 3 pixels but can vary in the image. The measurement of such a response in the center of the image gives often slightly different results on the boundary of the image.
The derivative of the SRF can be considered as a weighting function in a spatial convolution product, such as:

$$Y(x) = \int_0^L p(\chi)U(x-\chi)d\chi = \int_0^L p(x-\chi)U(\chi)d\chi$$

Or under discrete form :

$$Y_i = \sum_{j=1}^{N} p_{i-j}U_j\Delta x \quad \text{or} \quad \begin{bmatrix} Y_1 \\ Y_2 \\ . \\ . \\ Y_m \end{bmatrix} = \Delta x \begin{bmatrix} p_1 & p_2 & p_3 & .. & 0 \\ p_2 & p_1 & p_2 & & .. \\ p_3 & p_2 & p_1 & & \\ . & . & & . & p_2 \\ 0 & 0 & & p_2 & p_1 \end{bmatrix} \begin{bmatrix} U_1 \\ U_2 \\ . \\ . \\ U_m \end{bmatrix}$$

This space convolution is different from the time convolution previously implemented with solid sensors. Generally this weighting function is centered and symmetrical. The corresponding matrix is a band matrix.

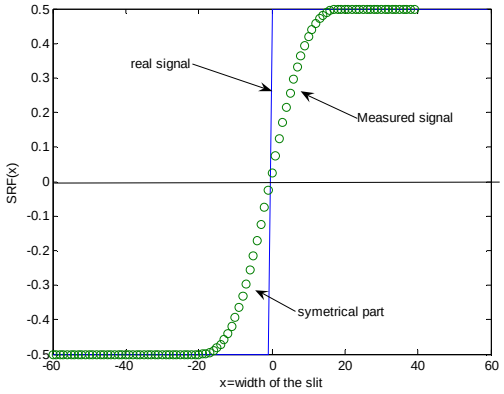

A-

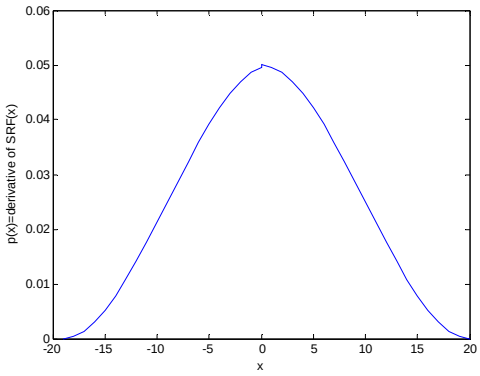

B-

Figure 3: A-Example of Slit Response Function and corresponding pixel positions, B-Derivative of the previous SRF function: $p(x)$ which is the kernel of the moving average applied to the signal.

1.3 Conclusion/ Synthesis of the first part

The previous list of possible errors and "unwanted noises" related to temperature field estimation is often frightening for the beginner. Maybe a rought synthesis can help the inexperienced user to start and practice the processing of such noisy and plentiful data.

Tree categories of noise can be globally considered:

-*the random noise* : with zero mean value is an unwanted perturbating noise but able to be processed with simples asumptions (related to the uniform covariance matrix).

-*the systematic errors*: (NUC, time derive, radiative parasitic effects, sensor positions ...) which must be fought, detected or bypassed by the experimenter.

-*the space and time convolutions and correlations* of the signal acting on the real time and space resolution limit. Such convolutions are considered as filters on the space and time signal. It will be generally difficult to obtain good estimations when the resolution limit is passed (even if deconvolution is a class of inverse problems). Such remark is remaining that the processing of a large amount of data must not give the illusion to dispose of the complete information about the phenomenon to be studied.

Other filters or convolutions will be considered in the second part of this text, devoted to the signal processing.

2. Thermal » processing of a 2D transient $T(x,y,t)$ field

From a 2D transient $T(x,y,t)$ field, and a heat transfer model (even simplified) is it often possible to estimate a resultant thermophysical properties field. The diffusion and convection transport modes can be considered in order to set out an identification model.The simple observation of the evolution of the temperature field can give the intuition of such phenomena (see the figure 4).

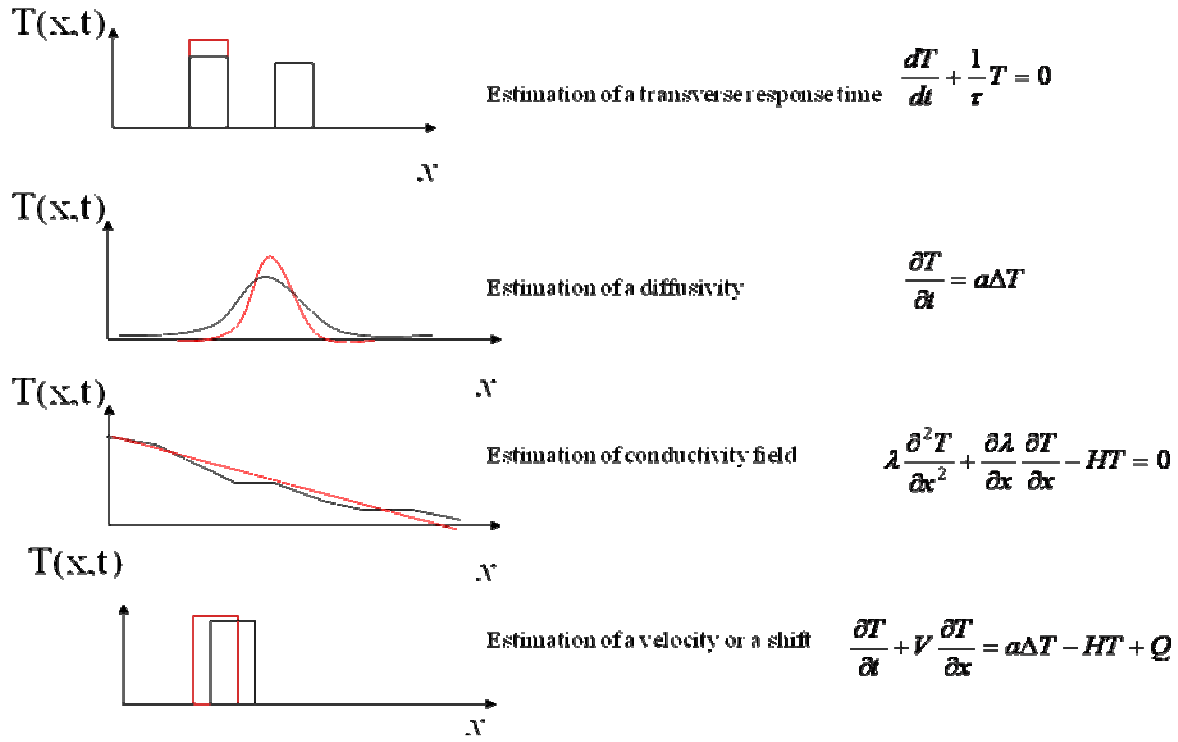

Figure 4. Illustration of the evolution of convective, in plane diffusive field, capacitive transverse field...

The processing of such fields needs of course to be aware of the previous “noise and perturbations” considerations about the temperature field recording. The random noise with a zero mean and a uniform and diagonal covariance matrix will generally be considered, but several aspects related to the “bad pixels”, the space or time correlation and the non regular time steps will appear on the following examples. Maybe, the first “natural”processing of such field is to try to set out the derivative (versus space or time) of the field. The space-derivative is often a mean to analyse the signal by considering the gradient of the signal (from displacement to stress in solid mechanics see [8]).

2.1 Strategies for the estimation of the time and space derivative of the signal :
The space or time derivation of noisy fields is a difficult task, because such operator is amplifying the random measurement noise, if no precaution is taken (see figure 5). A “filtering” is then necessary, but the risk is to lose a part of the original information. Several strategies will be here examined (the finite differences, the polynomial fit, the orthogonal basis decomposition and the convolution), in order to numerically implement the derivation of a dicrete signal.
In order to test these strategies the relaxation of an initial step such as:

$$T(x,t=0)=1 \text{ if } 0<x<b=L/2 \quad \text{and } T(x,t=0)=0 \text{ if } b=L/2<x<L$$

After a time t, the temperature field is relaxed (or filtered) by diffusion, and an approximation of the field is then:

$$T(x,t)=b/L+2/L\sum_{n=1}^{N}\frac{\sin(\alpha_n b)}{\alpha_n}\exp(-a{\alpha_n}^2 t)\cos(\alpha_n x)$$

with: $\alpha_n = n\pi / L$ and n,N finite integers.

Rigourously, the previous expression is a serie with N tending to infinity. A physical filter (due to the exponential term) is acting here and limiting the space-frequency content of the signal. The parameter which allows to control the filter is here the observation time. This observation time will be fixed in this section and only the space field will be considered.

The observed temperature is a vector obtained from the previous expression at regularly spaced space steps and a white gaussian noise is added.

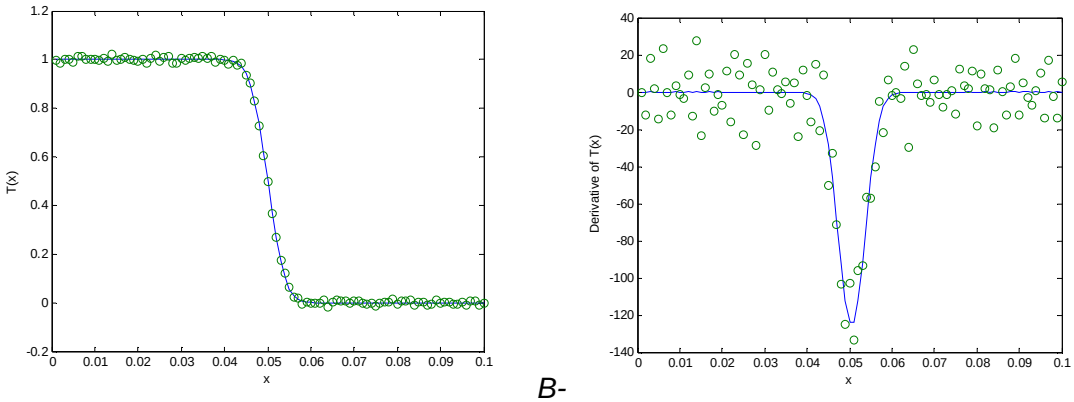

A- *B-*

Figure 5: A- Temperature field from the previous analytical expression at time $t=0.5s$; $a=10^{-5}$ m^2 s^{-1}; $b=L/2$; $L=0.1m$; (continuous line: real signal, 'o': discrete noisy signal); *B*-Derivative of the previous noisy signal by finite differences.

The initial gaussian noise is with zero mean and $\sigma=0.01$. The resulting noise is amplified by the derivation operation.

2.1.1 Finite differences

The finite difference approach used on figure 5 is generally presented at each space step i, as:

$$\hat{T}'_i = \frac{\hat{T}_{i+1} - \hat{T}_i}{\Delta x}$$

If it is assumed, that the relation between the observed temperature $\hat{T}_i$ and the real temperature T_i is:

$$\hat{T}_i = T_i + e_{T_i},$$

with e_{T_i} representing the random variable related to the gaussian noise, uniform whatever the position x_i. The asymptotic expansion around x_i is such as:

$$\hat{T}'_i = \frac{T(x_{i+1}) - T(x_i)}{\Delta x} + \varepsilon(x_{i+1}) + \frac{e_{Ti+1} - e_{Ti}}{\Delta x}$$

With:

$$\lim_{x \to x_i} \varepsilon(x) = 0$$

Two kinds of errors have then to be considered: the *approximation error* $\varepsilon(x_i)$ related to the rest of the asymptotic expansion and the *random error* related to the random variable e_{T_i}.

Unfortunately, when the space step Δx is tending to zero, the approximation error is effectively tending to zero, but the random error is tending to infinity!

The difference of two random variables is a linear operation which amplify the initial noise. In order to avoid such a difficulty, it is necessary to "filter" the signal or to project the discrete observed information in a basis of functions. One of the simplest basis of function can be a polynomial basis.

2.1.2 Polynomial fitting

From the same previous measurements, a polynomial fitting can be implemented such as:

$$T(x) = \sum_{n=0}^{N} \beta_n x^n$$

The estimation of the β_n parameters in vector: $\mathbf{B} = [\,\beta_1, \beta_2, \beta_3 .... \beta_n\,]^T$ can then be obtained by a linear least-square relation such as :

$$\mathbf{B} = \left(\mathbf{X}^t\mathbf{X}\right)^{-1}\mathbf{X}^t\hat{\mathbf{T}}$$

With:

$$\mathbf{X} = \begin{bmatrix} 1 & x_1 & {x_1}^2 \ldots \\ 1 & x_2 & {x_2}^2 \ldots \\ . & & \\ 1 & x_m & {x_m}^2 \ldots \end{bmatrix}$$

In order to minimize the distance:

$$\left\|\hat{\mathbf{T}} - \mathbf{XB}\right\| = \left(\hat{\mathbf{T}} - \mathbf{XB}\right)^T \left(\hat{\mathbf{T}} - \mathbf{XB}\right)$$

The construction of the derivative will then consist in considering the derivative of the polynomial function. The Matlab software is convenient in order to implement such calculations because the $\mathbf{X}^t\mathbf{X}$ matrix can be bad conditioned (Wandermonde matrix) and must be inversed with special precautions. One example of such processing is shown on the figure 6.

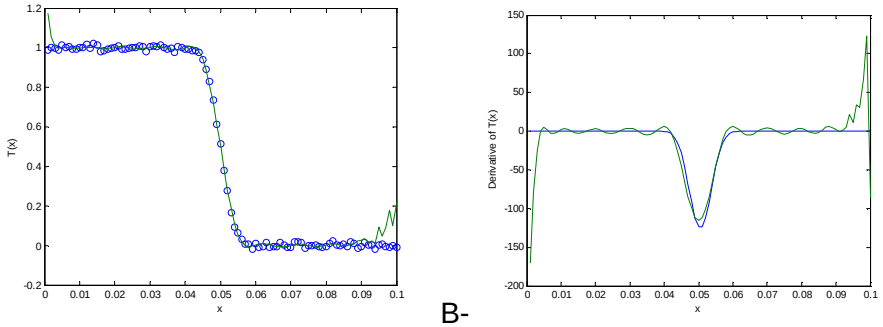

A- B-

Figure 6: A-polynomial fitting of the signal shown on figure 5. B- Derivation.

The chosen degree of the polynomial fitting is here: $N=30$. The number of observation points is 100.

Is shown here that the direct derivation of the estimated polynomial expression is giving a suitable continuous approximation in the considered domain. Approximation errors are occurring at the boundary of the domain if no precautions or assumptions are taken. One other strategy is to chose a basis "near from the considered physical phenomenon". Here, the ideal basis if the basis made of the Fourier cosine functions, because the cosine vectors are here verifying the boundary conditions (null derivative at $x=0$ and $x=L$) and are also the

eigenvectors of the diffusion phenomenon (eigenvectors of the Laplacian operator in Cartesian coordinates and adiabatic boundaries).

2.1.3 Fourier cosine basis

The same processing as the polynomial fitting can be considered with such an expression:

$$T(x) = \sum_{n=0}^{M} \beta_n \cos(\alpha_n x) \quad \text{with:} \quad \alpha_n = n\pi / L$$

The estimation of the parameter vector: $\mathbf{B} = [\beta_1, \beta_2, \beta_3 .... \beta_M]^T$ is then obtained by the same expressions as previously (in section 2.1.2), excepted that the $\mathbf{X}'\mathbf{X}$ matrix is orthogonal, and then very easy to be inverted. The covariance matrix related to the parameters is then as diagonal as the observable vector.

The result of the estimation is then, with 30 terms for the serie, illustrated on figure 7.

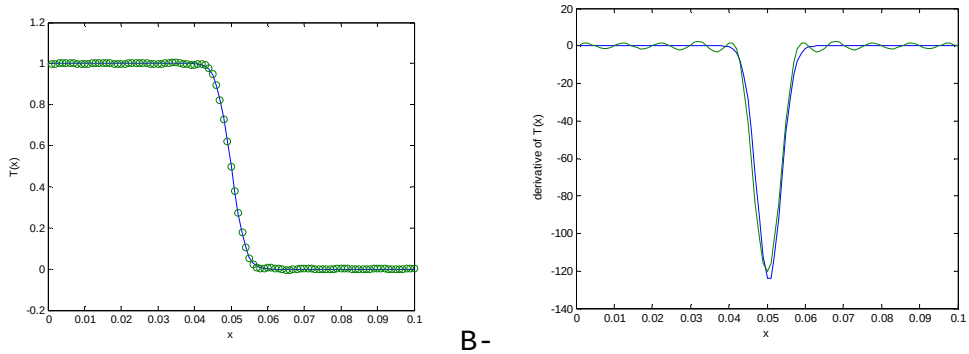

A- B-

Figure 7: A-Fourier fitting of the signal shown on figure 5. B- Derivation. The number of terms is $N=30$. The number of observation points is 100.

2.1.4 Filtering with a convolution kernel

The filtering is a usual operation in signal processing, which consist in weighting the signal with a moving average. It must be noticed that the observable signal himself is maybe previously filtered by the proper instrument. Such as explained in part 1. A new approximation of the signal can then be considered by $\widetilde{T}(x)$ such as :

$$\widetilde{T}(x) = \int_0^L p(\chi) T(x-\chi) d\chi$$

p(x) must be normed such as :

$$\int_0^L p(\chi) d\chi = 1$$

The derivative of $\widetilde{T}(x)$ is then conveniently considered by the commutability of the convolution product such as :

$$\frac{d\widetilde{T}}{dx}(x) = \int_0^L p(\chi) \frac{dT(x-\chi)}{dx} d\chi = \int_0^L T(\chi) \frac{dp(x-\chi)}{dx} d\chi$$

The discrete approximation of the derivative is then conveniently considered by a convolution with a « derived » kernel.

One very simple illustration is given on figure 8. The discrete convolution kernel of the filter is for example [1 2 1]/4 and an approximation of the convolution kernel for the derivation is then [1/2 0 -1/2]. It can be noticed that this "slight" convolution (affecting only a few number of neighbors and very similar to the finite difference method) allows to obtain good results with less effort.

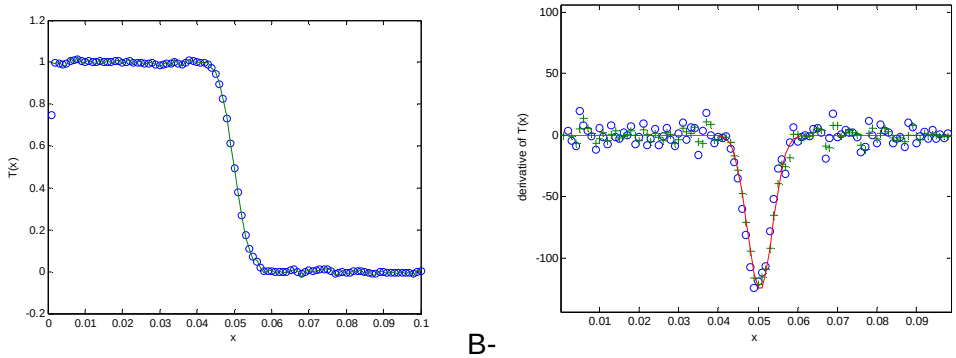

A- B-

Figure 8: A-Filtering of the signal shown on figure 5, with a convolution kernel: [1 2 1]/4 B-Derivation with a convolution kernel: [1/2 0 -1/2] (plot'o') and comparison with the finite difference derivative of the previously filtered signal (plot'+').

1.2.5 Singular value decomposition of the whole space and time signal

The previous methods consists in finding a compromise between the "approximation error" and the "filtering". The number of terms of the serie (or the rank of basis), or the width of the convolution kernel are biasing the signal if they are "used too far". A lot of other methods can be considered (for example more sophisticated regularisation technics, see **[9]**). When a large field must be processed the choice of the compromise between the filtering and the bias is made by trial and error.

The key point is the knowledge of the random noise (at the minimum the standard deviation). Often, the experiencer does not know the characteristic of the noise in his proper experience. It is then difficult to implement an optimal filtering of the signal.

One way to separate the "available signal" from the "random noise", when the experiencer has a great amount of space and time information, consists in implementing the singular value decomposition (SVD) of the $T(x,t)$ field, or the $\hat{T}(x_i,t_j)$ discrete observable matrix.

Applying the SVD to temperatures matrix $\hat{\mathbf{T}}$ yields

$$\hat{\mathbf{T}} = \mathbf{U}_{nxn}\Sigma_{nxn}\mathbf{V}_{nxm}{}^{T}$$

Where Σ is a sparse diagonal matrix as described below

$$\Sigma_{n\times m} = \left[\Sigma_{n\times n} \quad 0_{n\times(m-n)}\right]$$

So that finally the following truncated formulation of the SVD is commonly accepted

$$\hat{\mathbf{T}} = \mathbf{U}_{nxn}\Sigma_{nxn}\mathbf{V}_{nxm}{}^{T} = \sum_{k=1}^{n}\gamma_k\left(U_k.V_k{}^{T}\right)$$

Where the modes U_k and V_k are the column vectors of matrices $\mathbf{U}$ and $\mathbf{V}$ respectively, and the singular values γ_k are the diagonal elements of Σ_{nxn} arranged in descending order.
Such a decomposition of the global space/time field is offering a lot of advantages. First, the examination of the singular values γ_k allows to select the really available signal. Thermal phenomena are often related to diffusion problems (naturally filtered), with only a few available singular values.
The decomposition obtained with the reduced number of singular values is then offering a reduced representation of the field which allows a lot of possibilities (reduced computational effort for the further parameters estimations, low memory storage, new orthogonal basis and projection possibilities, see [10]).
In the case illustrated on figure 9, the SVD is allowing an optimal filtering without any previous knowledge about the random noise at any time. The finite differences derivative is then available without precautions.

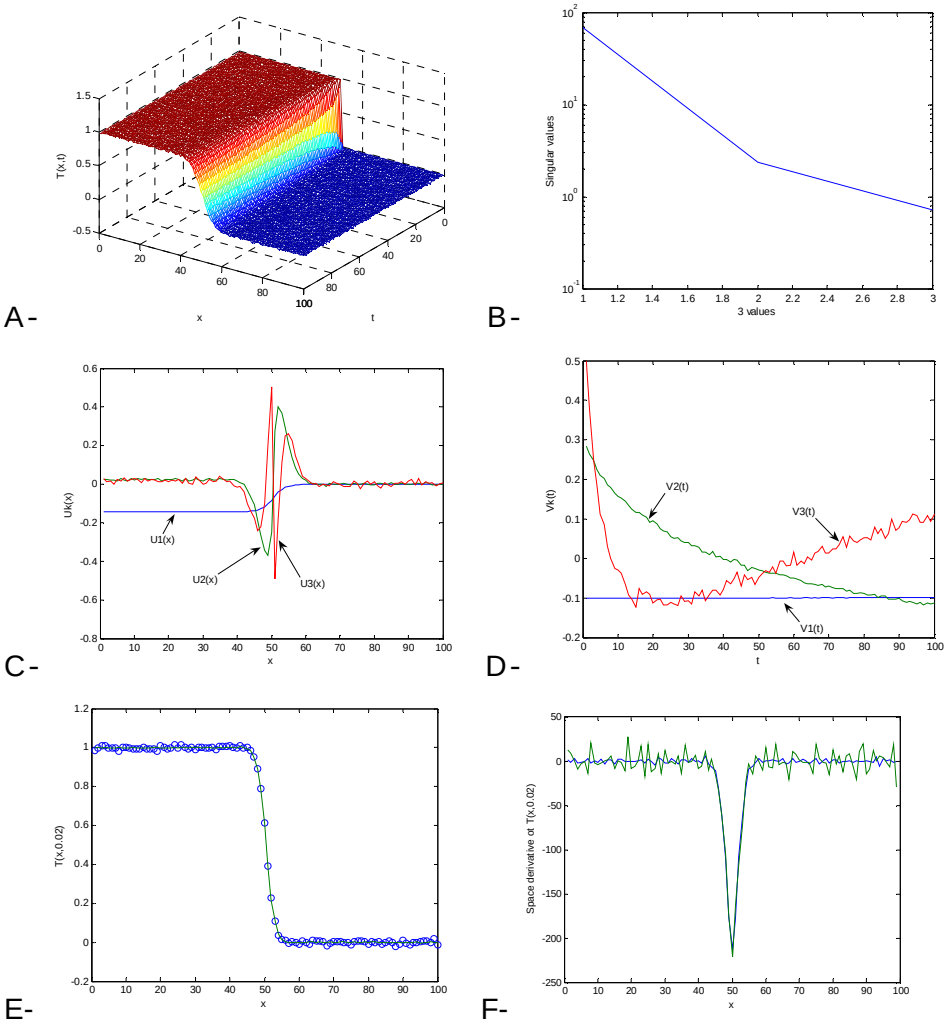

Figure 9: A- *T(x,t)* noisy temperature field (time extention from figure 5), B-3 first singular values,C-D-First $\mathbf{U}$ and $\mathbf{V}$ vectors, coming from the SVD decomposition, E- Reconstruction of the previous signal at time t=0.02s, with 3 term of the SVD decomposition.F- “Noisy” derivation of the previous signal (initial noisy observation) compared the finite differences derivative of the SVD reconstruction)

The previous example is showing that the transient situation even non-stationnary, is giving a greater amount of data than a unique image. The SVD decomposition is a mean to squize and to process the great amount of data quite with the same effort as in the stationnarycase.
It must be noticed that the orthogonal basis **U** is more reduced than the the basis of cosine functions used in section 2-1-4.

2.2 Estimation of a transverse diffusivity field from flash experiments (comparison of classical Non Destructive Evaluation methods):
2.2.1 Estimation with physical asymptotic expansion:
Non Destructive Evaluation (NDE) with infrared cameras consists generally to apply a heat pulse on a non homogeneous parallelepipedic slab and to process the temperature response $T(x,y,t)$ from one face of the sample (the front face or the rear face). The aim of such processing is to estimate some characteristics of the heterogeneities (structure, size, nature, position inside the sample…). The resolution of a general direct problem of transient heat transfer in a 3D heterogeneous geometry is often heavy and not convenient to implement such methods.
Here, thin samples with small heterogeneities such as the transfer is locally 1D (versus z direction), will be considered. One asymptotic expansion assuming that the heterogeneities fluctuations are small compared to the mean value of one thermophysical property of the sample yields a linear relationship, such as:

$$T(x,y,z,t) = q(x,y)\left(f(z,t,\beta_0) + \Delta\beta(x,y)\left.\frac{\partial f}{\partial \beta}\right|_{(z,t,\beta_0)} \right)$$

Where the functions $q(x,y)$ is the spatial distribution of energy coming from a flash excitation and $\Delta\beta(x,y)$ is the spatial thermophysical property variation(diffusivity, conductivity, thickness…). $q(x,y)$ and $\Delta\beta(x,y)$ have to be specified with a finite number of parameters which will be the object of the estimation procedure. Such procedure will then consists in processing the weighted sum of the images $T(x,y,z,t)$ where the weighting functions are the sensitivity functions $f(z,t,\beta_0)$ and $\left.\frac{\partial f}{\partial \beta}\right|_{(z,t,\beta_0)}$.
The temperature response of the front or the rear face of the sample will be recorded by a camera in order to estimate a map or a field of thermophysical properties. In the ideal case, the sample (a plane plate of small thickness L) is assumed to be thermally insulated and with a temperature field initially uniform ($T(x,y,z,t=0)=0$). If the heat transfer is supposed 1-D, then, the temperature response related to a unique location (x,y) corresponding to a pixel, to an instantaneous thermal pulse, is given (See [11]) on the front face $(z=0)$:

$$T(z=0,t) = \frac{Q}{\rho c L}\cdot\left(1 + 2\cdot\sum_{n=1}^{\infty}\exp\left(-\frac{n^2\cdot\pi^2\cdot a\cdot t}{L^2}\right)\right) = \frac{Q}{\rho c L}\, f\left(at/L^2\right)$$

Such expression is rather incomplete because the simplified assumptions (1D transfer, adiabacity…) can introduce a bias between modeling and experiment. Therefore, this expression is convenient to understand the different estimation procedure strategies. From the previous expression, the estimation problem of several parameters can be considered. Instead of the thermal diffusivity, the estimation problem of the sample thickness L, the thermal conductivity λ and the volumic heat capacity ρc can be considered. In each case, a reference approximated value of the parameter must be known (and noted: L_0, λ_0 and ρc_0) .

In many cases such reference values can be obtained by a previous global measurement. The following first order asymptotic expansions can be for example written for the front face, at each time t_i:

-If a thickness variation is to be estimated:

$$T(0,t_i) \approx \frac{Q}{\rho c L_0} f\left(\lambda t_i / \rho c {L_0}^2\right) - \frac{Q}{\rho c L_0}\frac{\Delta L}{L_0}\left(f\left(\lambda t_i / \rho c {L_0}^2\right) + 2t\left.\frac{\partial f}{\partial t}\right|_{(\lambda t_i / \rho c {L_0}^2)}\right)$$

-If a volumetric capacity variation is to be estimated:

$$T(0,t_i) \approx \frac{Q}{\rho c_0 L} f\left(\lambda t_i / \rho c_0 L^2\right) - \frac{Q}{\rho c_0 L}\frac{\Delta \rho c}{\rho c_0}\left(f\left(\lambda t_i / \rho c_0 L^2\right) + t\left.\frac{\partial f}{\partial t}\right|_{(\lambda t_i / \rho c_0 L^2)}\right)$$

-If a thermal conductivity variation is to be estimated:

$$T(0,t_i) \approx \frac{Q}{\rho c L} f\left(\lambda_0 t_i / \rho c L^2\right) + \frac{Q}{\rho c L}\frac{\Delta \lambda}{\lambda_0} t\left.\frac{\partial f}{\partial t}\right|_{(\lambda_0 t_i / \rho c L^2)}$$

It is very important to notice that in all previous cases, it is possible to replace the sensitivy functions $f(z=0,t,\beta_0)$ and $\left.\frac{\partial f}{\partial \beta}\right|_{(z,t,\beta_0)}$ by a linear combination of $f(z=0,t,\beta_0)$ and the time logarithmic derivative $t\left.\frac{\partial f}{\partial t}\right|_{(z=0,t,\beta_0)}$. It is then possible to implement a linear relationship such as:

$$T(0,t_i) \approx \beta_1 X_{\beta_1}(t_i) + \beta_2 X_{\beta_2}(t_i)$$

The functions $X_{\beta_j}(t_i)$ are the sensitivity functions of $T(0,t_i)$ to parameters β_j. Such functions are shown on figure 10. If other parameters combination estimation (such as thermal diffusivity estimation) is considered, the resulting sensitivity function will be a linear combination of functions f and $t\,(\partial f/\partial t)$.

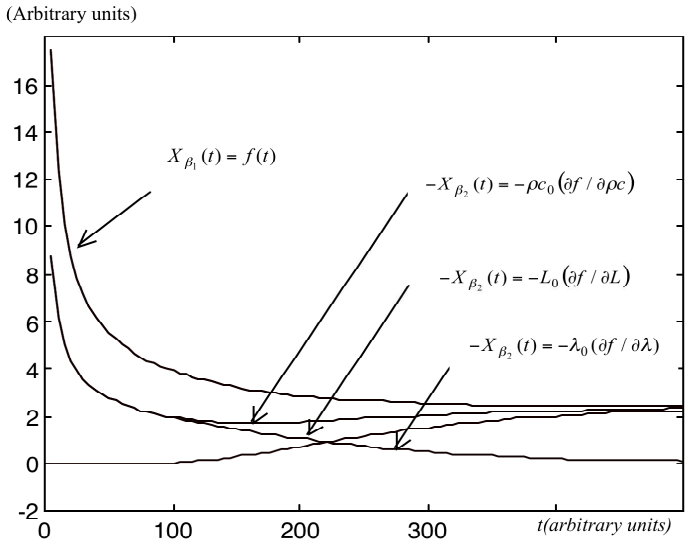

Figure 10 Sensitivity curves related to the 2-2-1 section.

The parameters β_j are defined in each estimation situation such as:

-If a thickness variation is to be estimated

$$\beta_1 = \frac{Q}{\rho c L_0} \quad \text{and} \quad \beta_2 = \frac{Q}{\rho c L_0}\frac{\Delta L}{L_0}$$

-If a volumetric capacity variation is to be estimated

$$\beta_1 = \frac{Q}{\rho c_0 L} \quad \text{and} \quad \beta_2 = \frac{Q}{\rho c_0 L}\frac{\Delta \rho c}{\rho c_0}$$

-If a thermal conductivity variation is to be estimated

$$\beta_1 = \frac{Q}{\rho c L} \quad \text{and} \quad \beta_2 = \frac{Q}{\rho c L}\frac{\Delta \lambda}{\lambda_0}$$

That is to say with matrix notation, considering the vectors and matrices:

$$\mathbf{T} = \left[T(0,t_1) \quad \cdots \quad T(0,t_N)\right]^t, \ \mathbf{X} = \begin{bmatrix} X_{\beta_1}(t_1) & \ldots & X_{\beta_1}(t_N) \\ X_{\beta_2}(t_1) & \ldots & X_{\beta_2}(t_N) \end{bmatrix}^t,$$

It yields under matrix notations:

$$\mathbf{T} = \mathbf{X}\begin{bmatrix} \beta_1 \\ \beta_2 \end{bmatrix}$$

If the measurement noise on each component of the experimental temperature vector $\hat{\mathbf{T}}$ is assumed with a constant standard deviation and not correlated, in the domain of validity of the previous asymptotic expansions, then, the optimal estimator of the parameters vector $\left[\hat{\beta}_1 \quad \hat{\beta}_2\right]$ is obtained by :

$$\begin{bmatrix} \hat{\beta}_1 \\ \hat{\beta}_2 \end{bmatrix} = \left(\mathbf{X}^t\mathbf{X}\right)^{-1}\mathbf{X}^t\hat{\mathbf{T}}$$

The linear approximation allows not only the estimation of the parameters, but also the confidence interval of this estimation to be studied. An intermediate stage is the covariance matrix of the estimation on the vector $\left[\hat{\beta}_1 \quad \hat{\beta}_2\right]$, given depending on the standard deviation of the temperature measurement noise σ_T :

$$\mathrm{cov}\begin{bmatrix} \hat{\beta}_1 \\ \hat{\beta}_2 \end{bmatrix} = \left(\mathbf{X}^t\mathbf{X}\right)^{-1}{\sigma_T}^2$$

The method can be used whatever the length of the vector $\hat{\mathbf{T}}$. These expressions can be implemented simultaneously with all of the pixels of the image. Thus, the matrix product $\mathbf{X}^t\hat{\mathbf{T}}$ can be incremented and consists in a real time weighting. The choice of the weighting is linked to the choice of the estimation strategy (estimation of L, ρc or λ). The terms of the sensitivity matrix are theoretically calculated with the references values or the averaged images. This sequential method considerably eases the problems of storage and images manipulation. It is very suitable for a simple Non Destructive Evaluation.

Moreover, *f(t)* can be "measured" on the data, because at each time step, the average of the image is a filtered approximation of *f(t)*. The computation of the logarithmic derivative of *f(t)* would then give a suitable method applicable without any idea about the knowledge of the nominal values of the thermophysical properties of the considered sample.

Unfortunately, the logarithmic derivative of this experimental signal is not easy with simple finite differences methods. In order to overcome such difficulties Shepard [12] proposed intuitively a logarithmic time-fitting each pixel signal and Rajic[13] to consider the SVD of the global data cube.

2.2.2 The logarithmic polynomial time-fitting [12]

In order to conveniently process the great amount of data provided by the flash NDE experiment, Shepard proposed to decompose the signal with a polynomial fitting, such as:

$$Ln(T(x,y,z=0,t)) = \beta_0(x,y) + \beta_1(x,y)Ln(t) + \beta_2(x,y)Ln^2(t) + \ldots$$

Such decomposition has no physical meaning because the new parameter vector is not related to a physical model, but the time-logarithmic derivative (considered by Shepard) appears to be very well correlated with the depth or thermophysical properties changes of the tested samples. The calculation of the logarithmic derivative is then taking the advantages related in section 2-1-2. It is also a very efficient and convenient method in order to reduce and manipulate the great amount of data (only N images corresponding to the degree of the polynomial expressions are to be manipulated).

2.2.3 The SVD decomposition ([13]-[10])

An other way to reduce the amount of data consists in considering the SVD of the information cube. Rajic [13] proposed the SVD decomposition (explained in 2.1.5) such as:

$$T(x,y,z=0,t)=\sum_{k=1}^{K}u_k(x)\gamma_k v_k(t)$$

Such data obtained from NDE experiments appears to be nicely reduced by 2 or 3 terms of the previous serie. Generally, the $\mathbf{U_1}$ vector (or $u_1(x)$ function) is giving a good approximation of the spatial energy distribution. The $\mathbf{V_1}$ vector (or $v_1(t)$ function) is related to *f(t)*. The $\mathbf{U_2}$ vector (or $u_2(x)$ function) is giving a good approximation of the defects localisation.

Bamford [10] proposed to compare the asymptotic expansion explained in the 2.2.1 section to the previous SVD decomposition. The slight differences are coming from the non-orthogonality of the functions in 2.2.1.

In fact all the methods presented in section 2.2 are very similar. They consist in projecting the data cube in a suitable basis of functions (physical or not) and then to try to process the signal with a physical model. In the next section, an other strategy is proposed. It consists in using the physical model in order to reduce or eliminate the non useful data (because nothing physically happens or because the sensor is providing a wrong signal).

2.3 Estimation of in-plane diffusivity field-Time-space correlation and elimination of the non useful data

Initally, in-plane characterization methods were related to modal methods (using cosine Fourier transform or projection on *cos(α_nx)* functions basis) allowing to estimate the thermal diffusivity of homogeneous anisotropic samples (see [14] ,[15] ,[16]). The main drawback of these methods is to be non adapted to heterogeneous samples, and also to consider only heat pulse or heat step heating responses.

When the sample is heterogeneous and when heat source terms can occur whatever the time or the space localization, it is difficult to set out analytical Fourier solutions, even polynomial fitting nor SVD decomposition (especially when the heating is random in time).

Nodal methods are then suitable and allow to consider other estimation strategies (see [17]). The local energy balance is then discrete and considered such as :

$$Fo_{i,j}\Delta T_{i,j}^{k}+\Phi_{i,j}^{k}=\delta T_{i,j}^{k}$$

with: $\Delta T_{i,j}^{k}=\left(T_{\mathrm{i+1,j}}^{k}+T_{\mathrm{i-1,j}}^{k}+T_{\mathrm{i,j+1}}^{k}+T_{\mathrm{i,j-1}}^{k}-4T_{i,j}^{k}\right)$ is proportional to the local Laplacian of the temperature field,

$Fo_{i,j}=\dfrac{a_{i,j}\Delta t}{\Delta x^2}$ Is the Fourier nondimensional local parameter related to the thermal diffusivity $a_{i,j}$; the pixel size Δx ; and the time step Δt .

$\Phi_{i,j}^{k}$ is a nodal source term which can occur randomly in space or time.

$\delta T_{i,j}^{k}=T_{i,j}^{k+1}-T_{i,j}^{k}$ is related to the discrete time-derivative.

It is then proposed to process the temperature field by looking only for the zone where there is a pure diffusion phenomenon (verifying only $Fo_{i,j}\Delta T_{i,j}^{k} = \delta T_{i,j}^{k}$). A criterion suitable to detect such zones is to consider the local correlation between the laplacian and the time derivative:

$$\rho_{i,j}^{F_t} = \frac{\sum_{F_t} \Delta T_{i,j}^{k} \delta T_{i,j}^{k}}{\sqrt{\sum_{F_t} \Delta T_{i,j}^{k\,2}} \sqrt{\sum_{F_t} \delta T_{i,j}^{k\,2}}}$$

where F_t is a temporal window such as: $F_t = [k, k+lt] with\ k \in [1, N-lt]$, k is the time step number and *lt* the width of the time window. If such a coefficient is near from 1, a diffusivity parameter is then estimable:

$$\frac{1}{Fo_{i,j}^{F_t}} = \frac{\sum_{F_t} \Delta T_{i,j}^{k} \delta T_{i,j}^{k}}{\sum_{F_t} \delta T_{i,j}^{k\,2}} = \frac{\rho_{i,j}^{F_t} \sqrt{\sum_{F_t} \Delta T_{i,j}^{k\,2}}}{\sqrt{\sum_{F_t} \delta T_{i,j}^{k\,2}}}$$

One example of temperature field processing is given on the figure 11 to 14.

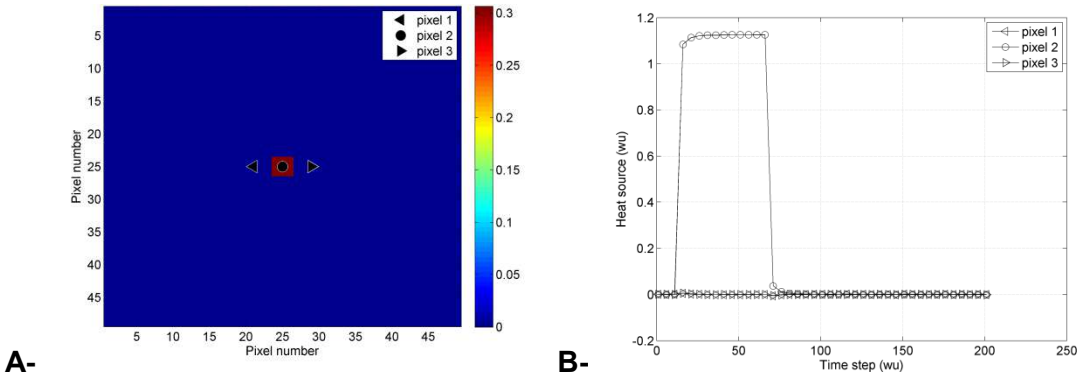

A- **B-**

Figure. 11 Source term A- Position of the hot spot B- Time evolution for 3 pixels in the center of the image

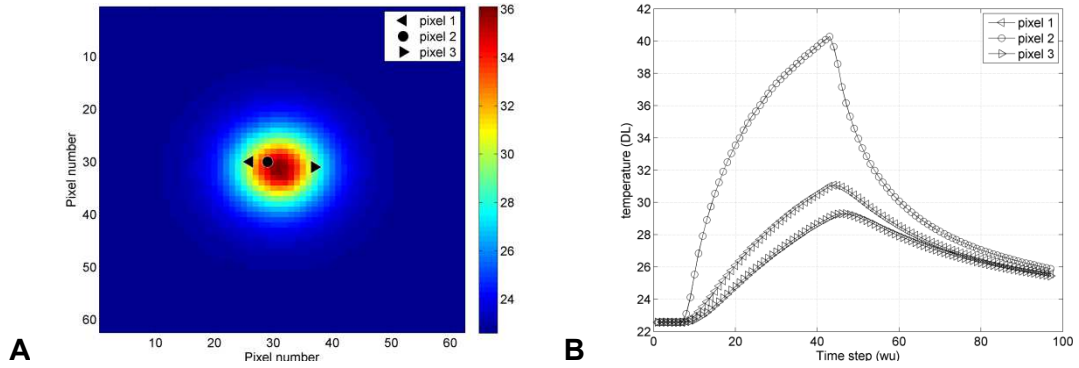

A **B**

Figure. 12 Temperature response A- Temperature field at t = 55 wu (without unit), B- Evolution of several pixels in the center of the image

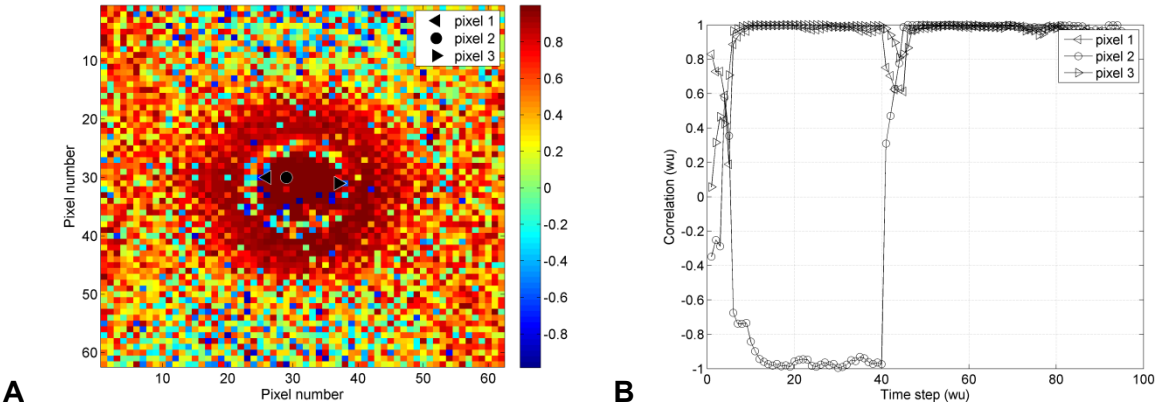

Figure.13 Correlation coefficients calculated for Ft =4. A- Field at t = 55 wu (just after the heat step) B- Time-evolution for3 pixels et the center of the image.

The field of correlation coefficient illustrated on figure 13 are showing the zones where the thermal diffusivity ois able to be estimated (correlation near from 1) and the zone where no estimation is possible.

This knowledge of the correlation field allow to estimate the diffusivity only in the suitable area (see figure 14).

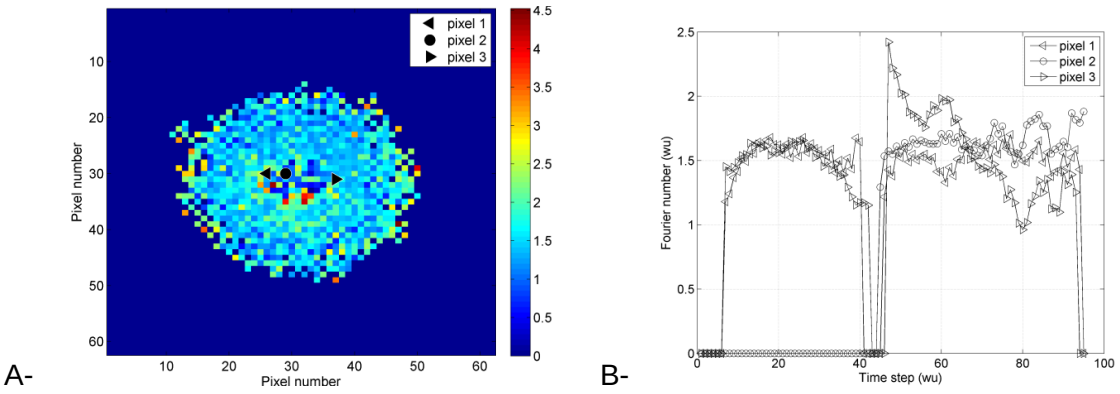

Figure 14: Estimation of the reduced diffusivity A- Field obtained from the whole information cube B- Quasi instantaneous estimation (window of 4 time steps).

From figure 15 it is interesting to remark that the “physical” correlation process allow to discriminate the zone where there is a pure diffusion phenomenon from the zone where there is a source term from also the zones where nothing appear or maybe the pixel are dead. This processing can then sometimes allow to partly overcome the processing and the considerations explained in the part 1. Especially when the signal is very noisy, the simple consideration of correlations can help to discriminate the areas where a source term or a purely diffusive relaxation appear.

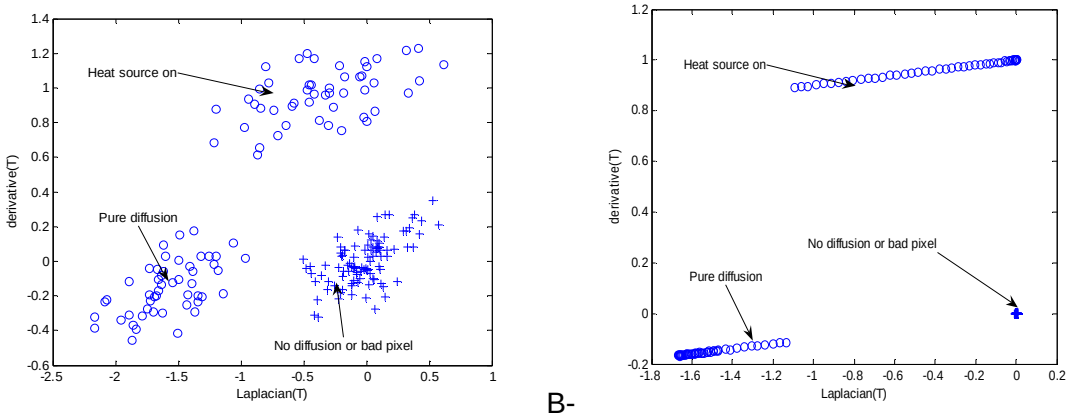

A- B-

Figure 15 Study of the correlation between Laplacian and time derivative for several pixels ('o' pixel with or without source term with diffusion, '+' pixel where no diffusion appear or "bad pixel". A- From noisy signal, B-From less noisy signal.

3 Conclusion:

The time-space thermal signal is offering a great amount of data which must be processed from several points of views. First, the different kinds of noise and bias (random, systematic and space and time correlations) coming from the instrument must be analysed and understood. Then several strategies are available in order to process the signal in relation with a physical model. Often the main strategy will consist in projecting the signal in a function basis which can come from intuition, statistical processing or physical analysis. This projection is advantageous in order to filter the random noise, to reduce the great amount of data and to conveniently manipulate and estimate the parameters. But the projection is not always the most suitable strategy. The direct condideration of a physical model will allow to eliminate or discriminate the data correlated or not with a chosen physical phenomenon (one example has been evocated with the estimation of a thermal diffusivity field).

References:

[1] B. Bourouga, V. Goizet, J.-P. Bardon, Les aspects théoriques régissant l'instrumentation d'un capteur thermique pariétal à faible inertie, International Journal of Thermal Sciences 39 (1) (January 2000) 96–109.

[2] J.L. Battaglia, J.C. Batsale, Estimation of heat flux and temperature in a tool during turning, Inverse Probl. Eng. 8 (2000) 435– 456.

[3] Gaussorgue G., Infrared thermography, 1994, Chapman et al, London.

[4] Maldague X.P.V., Theory and Practice of Infrared Technology for Nondestructive Testing, John Wiley & sons, Inc., 684 p, 2001.

[5] Balageas D., Delpech P., Boscher D., Deom A., "New developments in stimulated infrared thermography applied to non destructive evaluation of laminates", Review on

Progress in Quantitative Non-Destructive Testing, ED Thompson and Chimienti (Plenum Press, New York, 1991, Vol 10 A, pp 1073-1081.

[6] Batsale JC, Chrysochoos A, Pron, H., Watrisse B., 2011, Analyse thermographique du comportment des matériaux, in Mesure de champs et identification en mécanique des solides, hermes, Lavoiser,

[7] Pradere C., Clerjaud L., Dihlaire S. ,JC Batsale, 2011, High speed heterodyne infrared thermography applied to thermal diffusivity identification, Rev Sci. Instrum, 82, 054901

[8] Feissel P.., 2011, Du déplacement à la déformation, in Mesure de champs et identification en mécanique des solides, hermes, Lavoiser,

[9] Thikonov A. and Arsenine V., 1977 Solutions for ill posed problems, Winston and Sons, Washington.

[10] Bamford M., Batsale J.C., Fudym O., Nodal and Modal Strategies for longitudinal Thermal Diffusivity Profile Estimation. Application to the non-destructive Evaluation of SiC/SiC composites under uniaxial tensile tests, Infrared Physics and technology (2008), Volume 52, Issue 1, January 2009, Pages 1-13.

[11] Parker WJ, Jenkins, W., Abott J.., 1961 “Flash method of determining thermal diffusivity, Heat capacity and thermal conductivity”, Journal Appl. Phys., vol 32, No 9, pp 1679-1684,

[12] S.M. Shepard, Y.L. Hou, T. Ahmed and J.R. Lhota, “Reference-free Interpretation of FlashThermography Data”, Insight, Volume 48, No. 5, British Institute of NDT, May 2006, pp.298-307.

[13] Rajic N., Principal component thermography for flaw contrast enhancement and flaw depth characterisation in composite structures, Composite Structures Volume 58, Issue 4, December 2002, Pages 521-528

[14] Philippi I., Batsale J.C., Maillet D., Degiovanni A., Measurement of thermal diffusivity through processing of infrared images, Rev. Sci. Instrum. 66(1) 1995, 182-192.

[15] Krapez JC, Spagnolo L., FrieB M., Maier H.P., Neuer, Measurement of in-plane diffusivity in non-homogeneous slabs by applying flash thermography, International Journal of Thermal Sciences 43 (2004) 967-977.

[16] Souhar Y., 2011, Caractérisation thermique de matériaux anisotropes à hautes températures, INPL Doctorate Thesis, Nancy.

[17] Pradère C., Morikawa J., Toutain J., Batsale J.C., Hayakawa E., Hashimoto T., Microscale thermography of freezing biological cells in view of cryopreservation, QIRT Journal, VOL 6/1 - 2009 - pp.37-61 - doi:10.3166/qirt.6.37-61